

## Supporting Information

### Porous Al<sub>11</sub>Ce<sub>3</sub> intermetallics as effective sulfur host networks for stable lithium–sulfur batteries

Can Mi,<sup>‡,a</sup> Zigang Wang,<sup>‡,a</sup> Shenbo Yang,<sup>b</sup> Xijun Liu,<sup>c</sup> Yichao Wang,<sup>\*,d</sup> and Zhifeng Wang <sup>\*,a</sup>

a. “The Belt and Road Initiative” Advanced Materials International Joint Research Center of Hebei Province, School of Materials Science and Engineering, Hebei University of Technology, Tianjin 300401, China

b. Hongzhiwei Technology (Shanghai) Co., Ltd., Shanghai 201206, China

c. School of Resources, Environment and Materials, Guangxi University, Nanning 530004, China.

d. School of Science, RMIT University, Melbourne VIC 3001, Australia

‡ Can Mi and Zigang Wang contributed equally.

\* Corresponding authors.

Yichao Wang (E-mail: [yichao.wang@rmit.edu.au](mailto:yichao.wang@rmit.edu.au))

Zhifeng Wang (E-mail: [wangzf@hebut.edu.cn](mailto:wangzf@hebut.edu.cn))

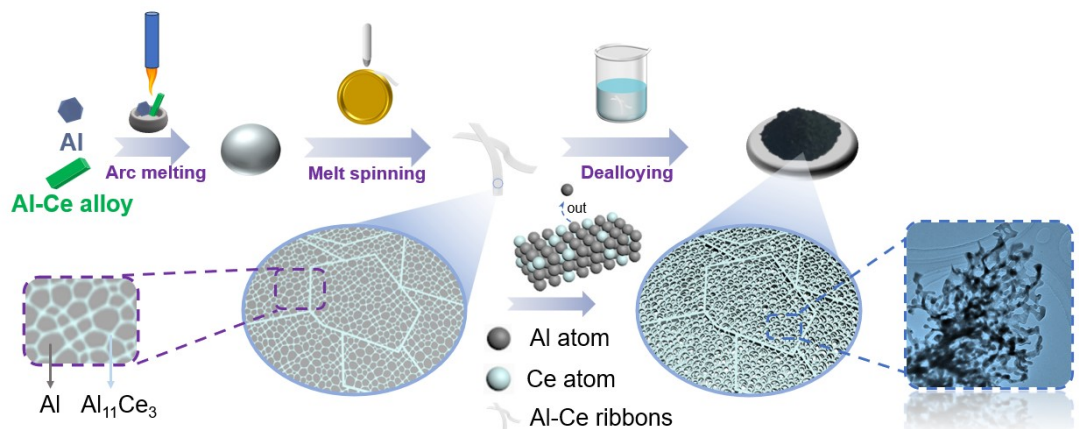


Fig. S1. Schematic diagram of the synthesis route.

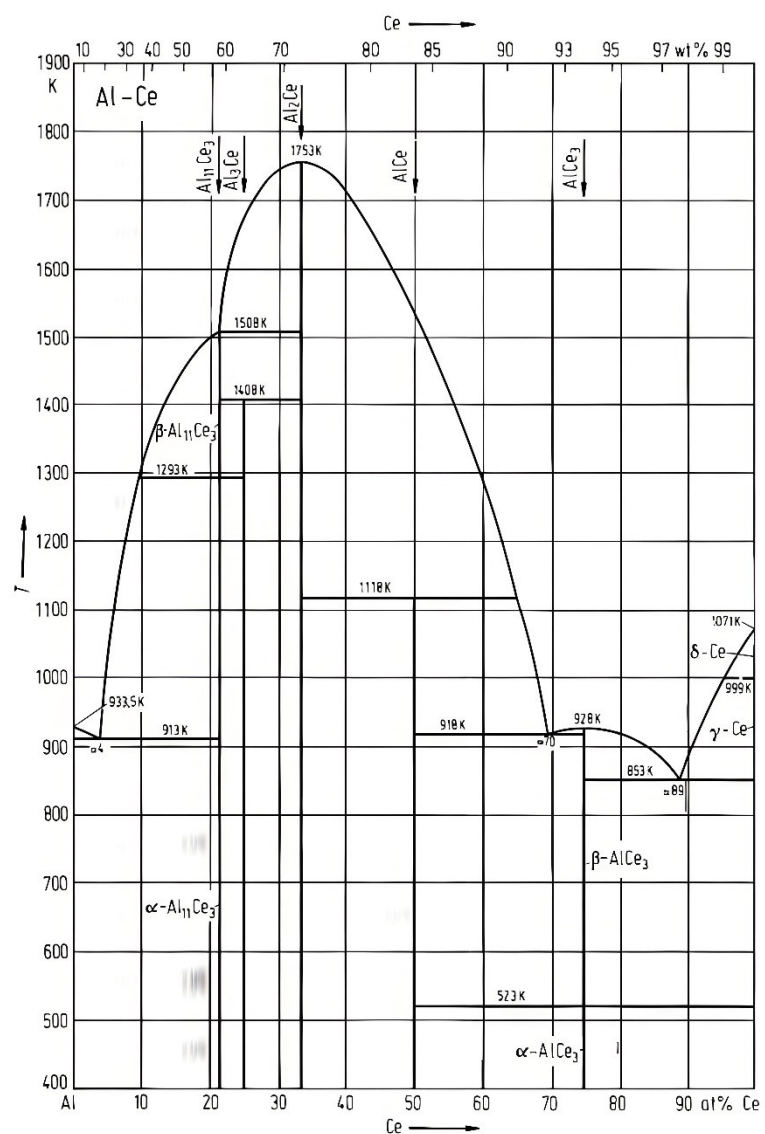


Fig. S2. Al-Ce binary phase diagram.

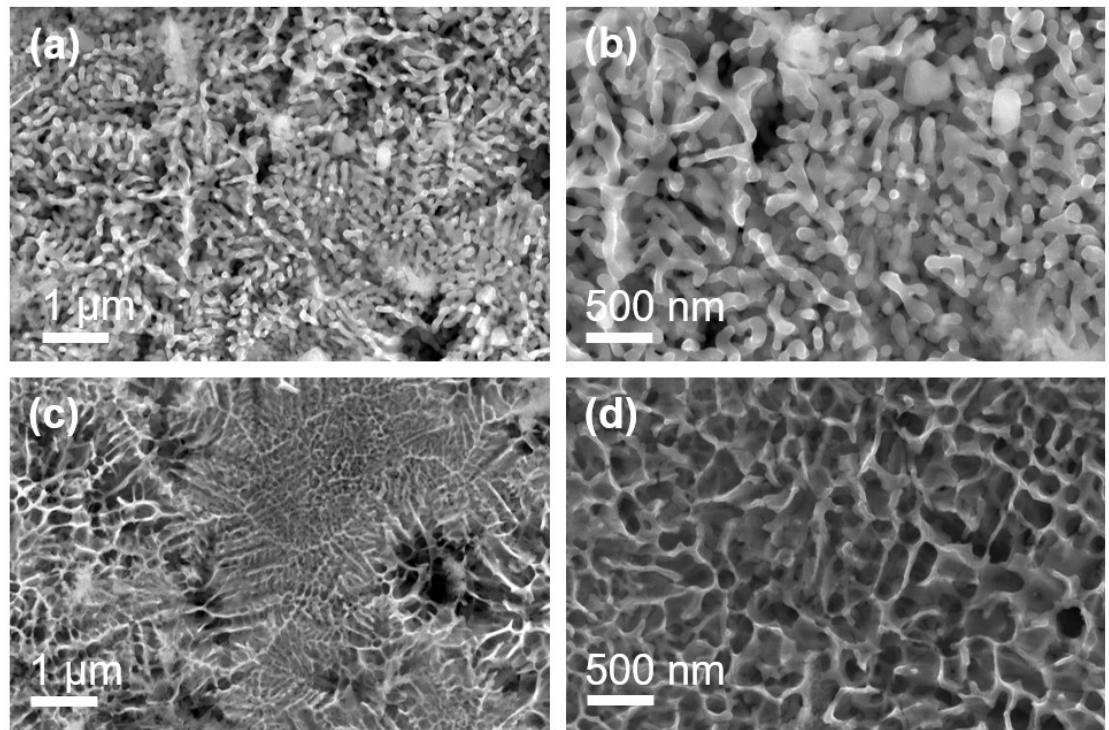


Fig. S3. SEM images of (a,b) D-Al<sub>90</sub>Ce<sub>10</sub> and (c,d) D-Al<sub>98</sub>Ce<sub>2</sub>.

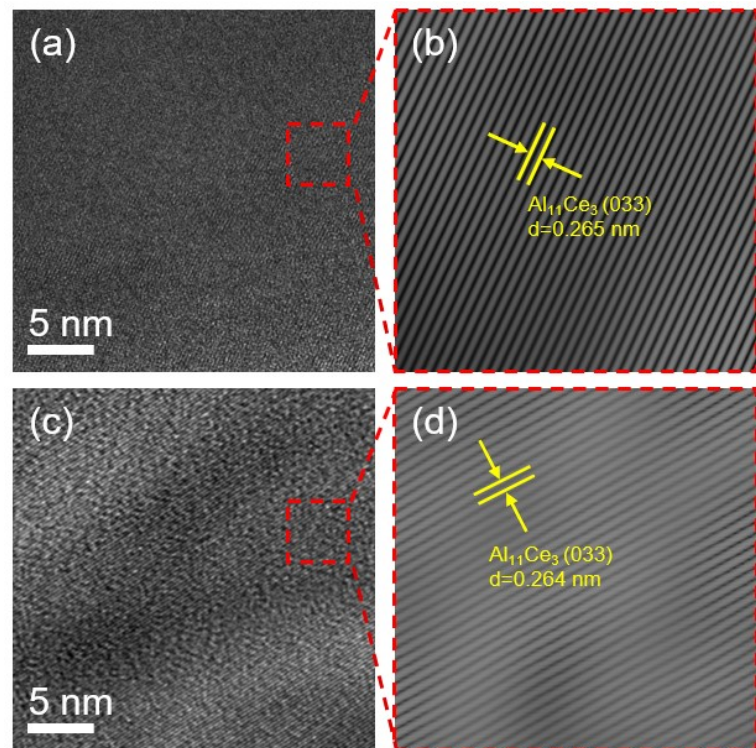


Fig. S4. HR-TEM images of D-Al<sub>90</sub>Ce<sub>10</sub> (a,b) and D-Al<sub>98</sub>Ce<sub>2</sub> (c,d).

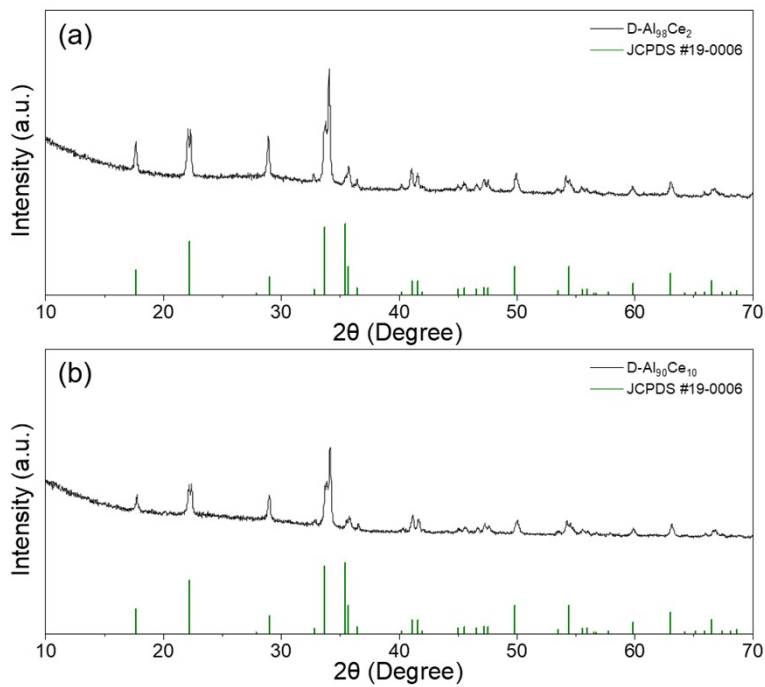


Fig. S5. XRD pattern of (a)  $D\text{-Al}_{98}\text{Ce}_2$  and (b)  $D\text{-Al}_{90}\text{Ce}_{10}$ .

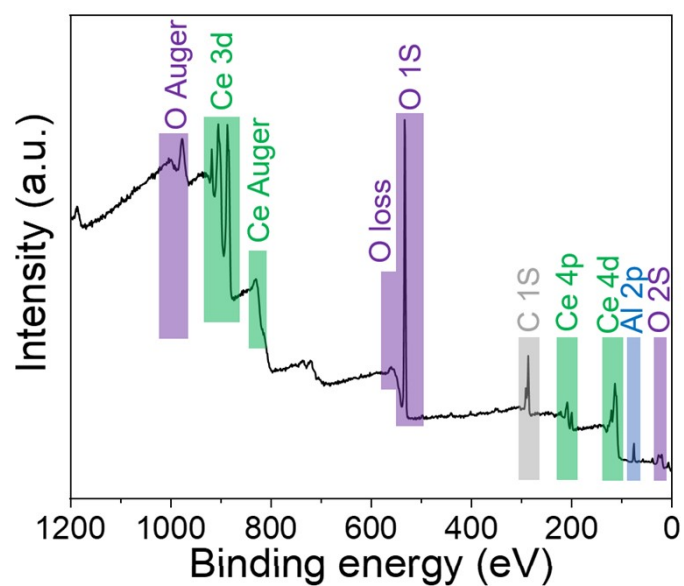


Fig. S6. XPS survey spectra of D-Al<sub>96</sub>Ce<sub>4</sub>.

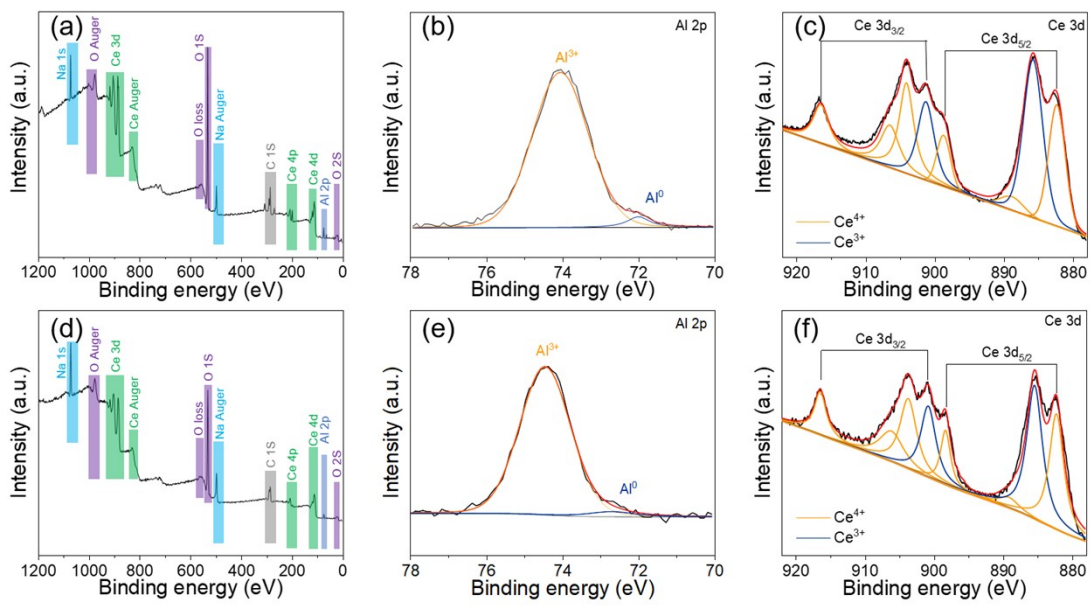


Fig. S7. (a-c) XPS spectra of D-Al<sub>98</sub>Ce<sub>2</sub>: (a) XPS survey spectra, (b) Al 2p, (c) Ce 3d; (d-f) XPS spectra of D-Al<sub>90</sub>Ce<sub>10</sub>: (d) XPS survey spectra, (e) Al 2p, (f) Ce 3d.

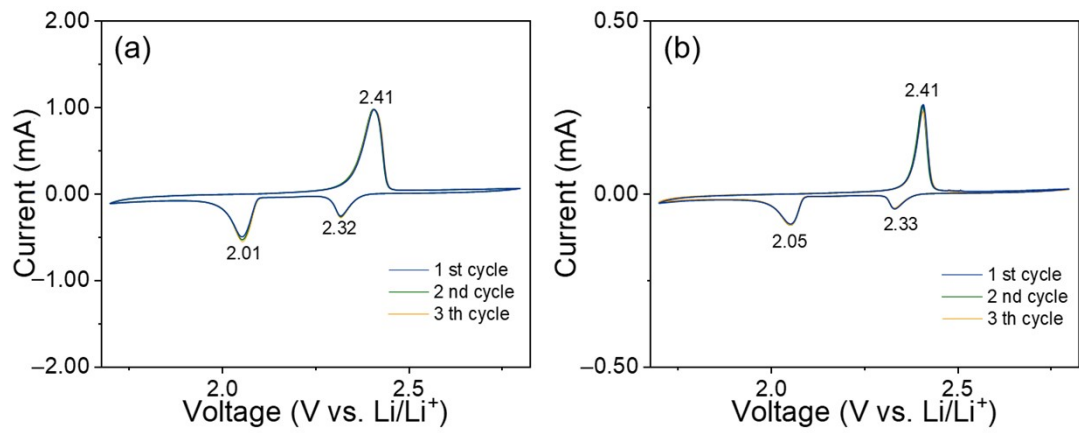


Fig. S8. CV profiles of (a) S@D-Al<sub>90</sub>Ce<sub>10</sub> and (b) S@D-Al<sub>98</sub>Ce<sub>2</sub> cathode at 0.1 mV s<sup>-1</sup>.

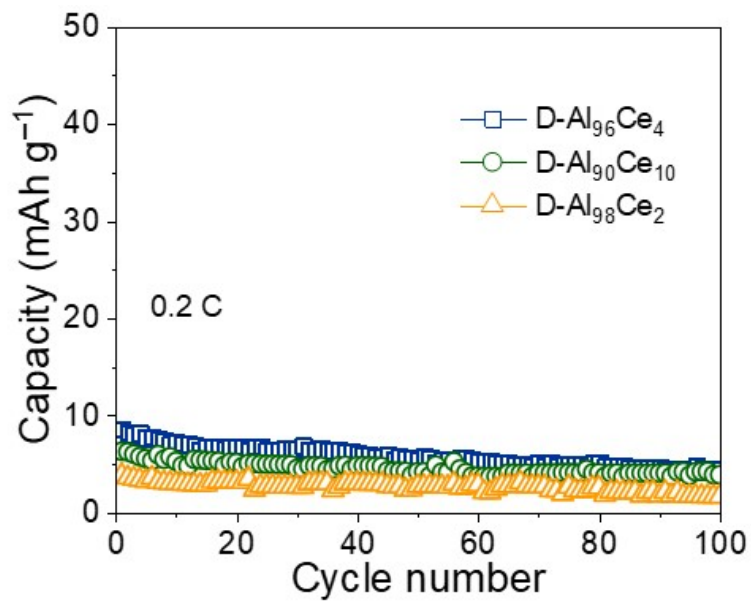


Fig. S9. Cycling performance of the D-Al<sub>98</sub>Ce<sub>2</sub>, D-Al<sub>96</sub>Ce<sub>4</sub>, and D-Al<sub>90</sub>Ce<sub>10</sub> electrodes at the current density of 0.2 C

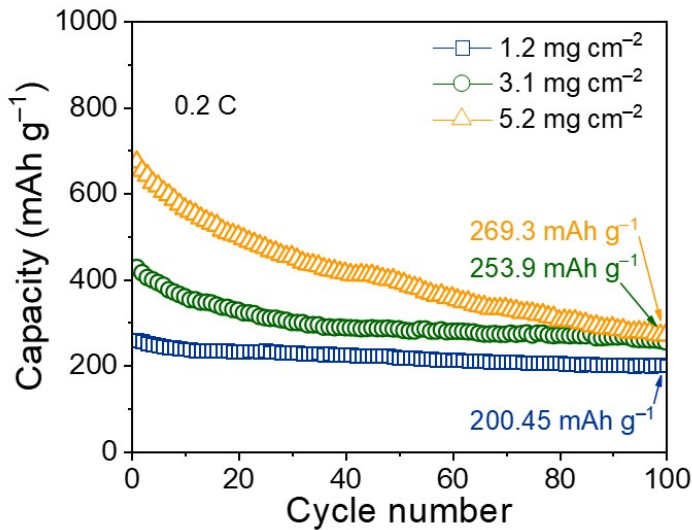


Fig. S10. Cycling performance of S@D-Al<sub>96</sub>Ce<sub>4</sub> with different sulfur loadings from 1.2 to 5.2 mg cm<sup>-2</sup> at 0.2 C.

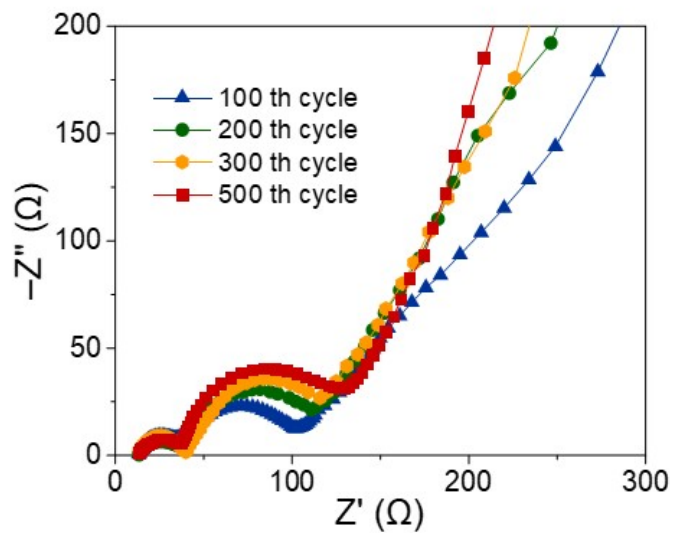


Fig. S11. EIS curves of S@D-Al<sub>96</sub>Ce<sub>4</sub> after cycling at 1 C current density for different cycles.

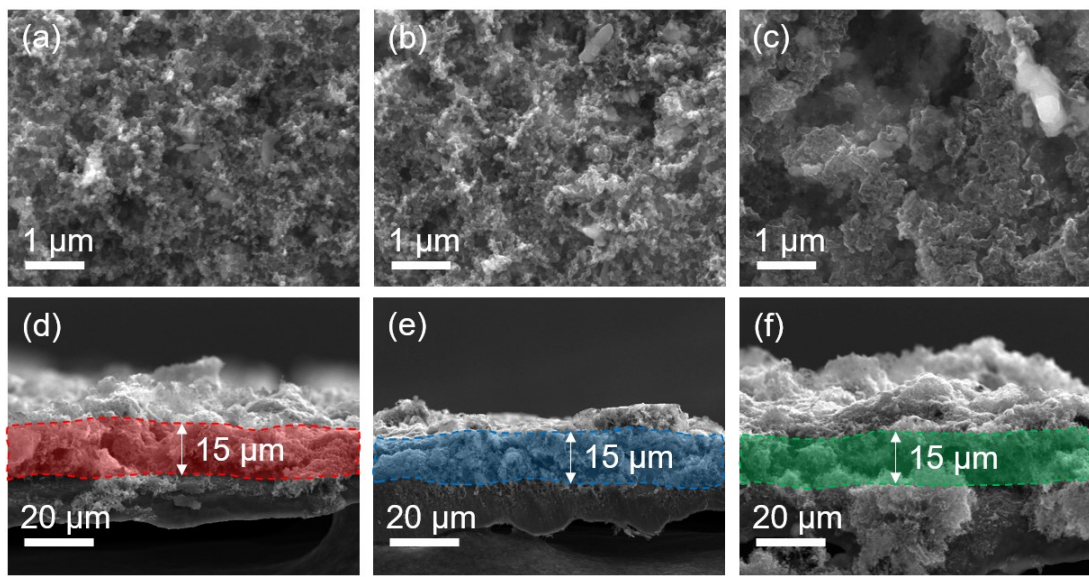


Fig. S12. SEM images of fresh (a) S@D-Al<sub>96</sub>Ce<sub>4</sub>, (b) S@D-Al<sub>90</sub>Ce<sub>10</sub>, and (c) S@D-Al<sub>98</sub>Ce<sub>2</sub> cathodes.

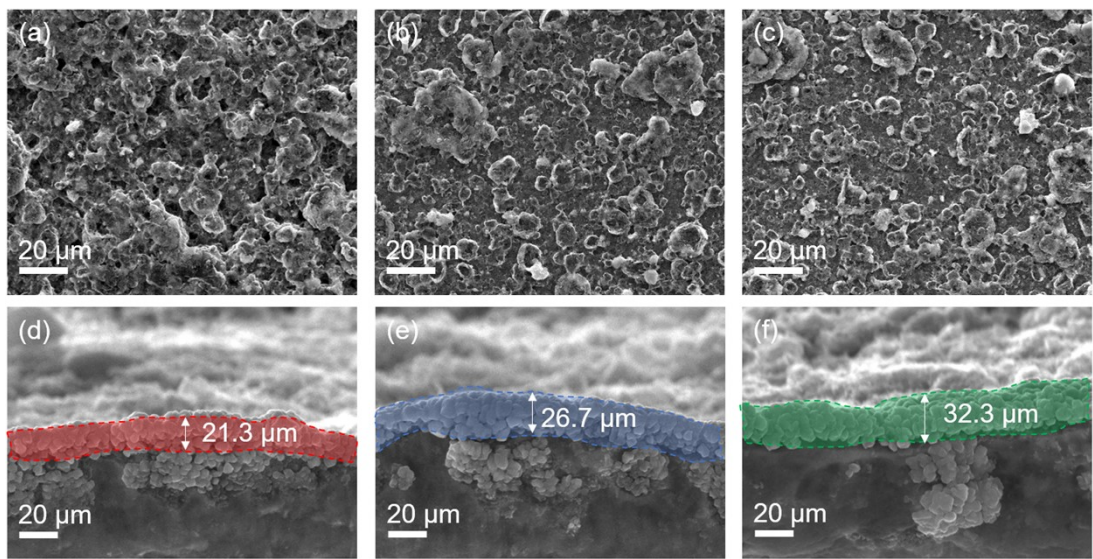


Fig. S13. SEM images of (a) S@D-Al<sub>96</sub>Ce<sub>4</sub>, (b) S@D-Al<sub>90</sub>Ce<sub>10</sub>, and (c) S@D-Al<sub>98</sub>Ce<sub>2</sub> cathodes after cycling at 0.2 C for 100 cycles.

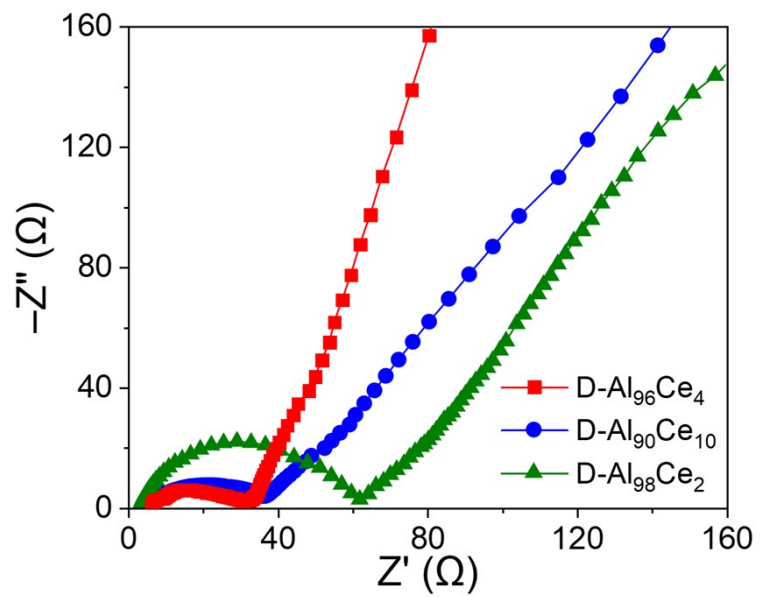


Fig. S14. EIS spectra of symmetric cells with D-Al<sub>98</sub>Ce<sub>2</sub>, D-Al<sub>96</sub>Ce<sub>4</sub>, and D-Al<sub>90</sub>Ce<sub>10</sub> electrodes

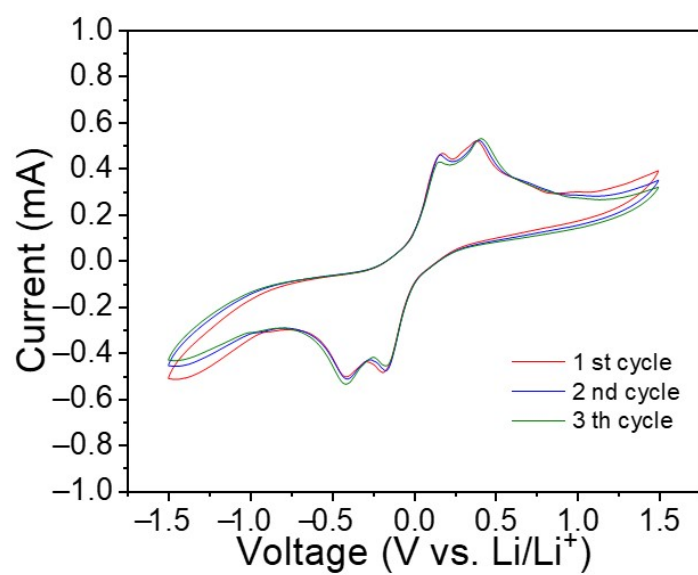


Fig. S15. CV curves of symmetric cells with D-Al<sub>96</sub>Ce<sub>4</sub> electrodes.

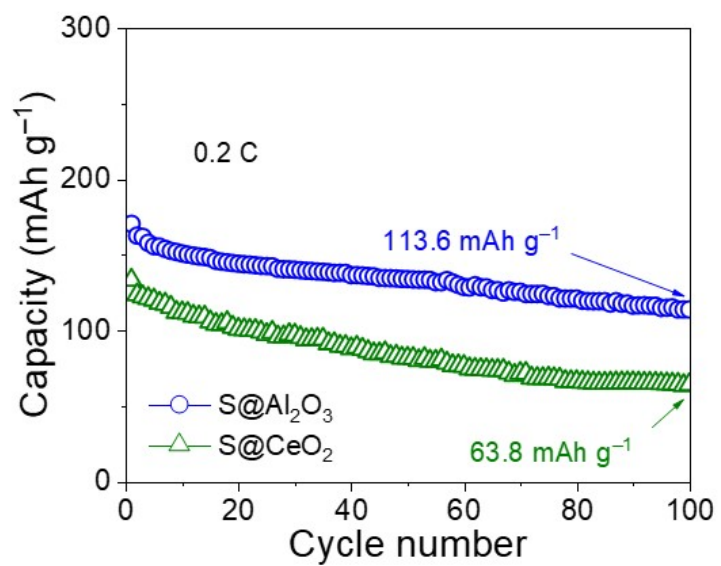


Fig. S16. Cycling performance of the S@Al<sub>2</sub>O<sub>3</sub> and S@CeO<sub>2</sub> cathodes at the current density of 0.2 C

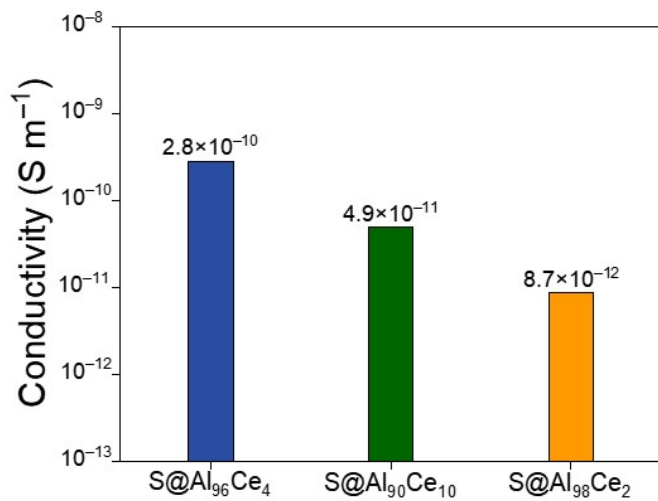


Fig. S17. Electrical conductivity of the  $\text{S@D-Al}_{98}\text{Ce}_2$ ,  $\text{S@D-Al}_{96}\text{Ce}_4$ , and  $\text{S@D-Al}_{90}\text{Ce}_{10}$  cathodes.

Table S1.  $R_{ct}$  values of EIS curves of different samples.

Sample	$R_{ct}$
S@D-Al <sub>96</sub> Ce <sub>4</sub>	53.3
S@D-Al <sub>90</sub> Ce <sub>10</sub>	54.1
S@D-Al <sub>98</sub> Ce <sub>2</sub>	83.5

Table S2.  $R_{ct}$  values of EIS curves of S@D-Al<sub>96</sub>Ce<sub>4</sub> with different cycles.

Cycle number	$R_{ct}$
100	61.7
200	70.8
300	75.7
500	89.8

Table S3 Comparison of electrochemical performance.

Material	Current density ( $\text{C}$ )	Cycle	Reversible capacity ( $\text{mAh g}^{-1}$ )	Reference
$\text{CeO}_2@\text{CNT/S}$	0.2	100	723	S1
$\text{CeO}_{2-x}\text{-CNT/S}$	0.5	600	877	S2
$\text{Zn}@\text{NPC-CeO}_2\text{-2}$	2	200	569.3	S3
$\text{Al}_2\text{O}_3@\text{C}$	0.1	200	302	S4
$\text{g-C}_3\text{N}_3/\text{CNTs}$	1	500	803.4	S5
$\text{V}_2\text{O}_3@\text{C-CNTs}$	0.5	500	715.4	S6
$\text{Co}_1\text{-CoS}_2@\text{CNT}@C$	1	500	555.8	S7
$\text{S}@\text{D-Al}_{96}\text{Ce}_4$	0.2	100	204.83	This work
	1	500	140	

## References

- S1. D. J. Xian, C. X. Lu, C. M. Chen and S. X. Yuan, *Energy Storage Mater.*, 2018, 10, 216-222.
- S2. Y. L. Xing, M. A. Zhang, J. Guo, X. Y. Fang, H. G. Cui, X. Q. Hu and X. Y. Cao, *J. Solid State Chem.*, 2022, 316, 123642.
- S3. W. J. Feng, J. Z. Chen, Y. P. Niu, W. Zhao and L. Zhang, *J. Alloys Compd.*, 2022, 906, 164341.
- S4. Y. C. Huang, C. C. Wu and S. H. Chung, *ChemSusChem*, 2024, e202402206.
- S5. W. Dong, Y. F. Guo, W. B. Wang, X. D. Hong, X. C. Xu, F. Yang, M. Y. Zhao, X. Zhang, D. Shen and S. B. Yang, *J. Energy Storage*, 2025, 110, 115256.
- S6. L. N. Jin, B. Z. Li, X. Y. Qian, S. L. Zhao and H. X. Xu, *J. Alloys Compd.*, 2025, 1010, 178108.
- S7. Y. Y. Zheng, M. Y. Xu, Y. H. Jin, Y. N. Mao, X. Zhang and M. Q. Jia, *J. Energy Storage*, 2025, 107, 115015.